Magnetic properties and instability phenomena in doped Euo

A. Mauger, C. Godart, M. Escorne, J.C. Achard, J.P. Desfours

Classification
Physics Abstracts
75.30 — 75.10 — 71.40

MAGNETIC PROPERTIES AND INSTABILITY PHENOMENA IN DOPED EuO

A. MAUGER[+], C. GODART[++], M. ESCORNE[+], J. C. ACHARD[++] and J. P. DESFOURS*

[+]CNRS Laboratoire de Physique du Solide, 1 pl. A. Briand 92190 Bellevue-Meudon

[++]CNRS ER 209 Equipe de Chimie Métallurgique et Spectroscopie des Terres Rares
1 pl. A. Briand, 92190 Bellevue-Meudon

*C.E.E.S. Université des Sciences et Techniques du Languedoc, 34060 Montpellier

(*Reçu le 27 avril 1978, révisé le 16 juin 1978, accepté le 22 juin 1978*)

Résumé. — Nous avons étudié l'influence de la concentration de porteurs libres sur les propriétés magnétiques de monocristaux de EuO. L'accroissement des concentrations électroniques à partir de EuO quasi stœchiométrique a été obtenu par écart à la stœchiométrie (EuO riche en Eu) et par dopage (EuO dopé à 2 % en Gd). L'aimantation des échantillons massifs caractérisés par des mesures de transport a été mesurée avec un magnétomètre vibrant. Pour les faibles dopages, les courbes d'aimantation ne diffèrent pas de celle donnée par la loi de Brillouin, avec une température de Curie de 69,4 K. Au contraire, pour l'échantillon très dopé au Gd, T_c atteint 143 K et l'aimantation réduite est plus petite que celle prévue par la loi de Brillouin. Nous proposons un modèle prenant en considération à la fois l'interaction de super-échange responsable des propriétés magnétiques de EuO isolant, et l'échange indirect dû aux électrons de conduction pour les échantillons semiconducteurs et métalliques. Le point essentiel est que, contrairement aux modèles classiques, nous tenons compte de la statistique des porteurs, i.e. la séparation des sous-bandes de spin et l'élargissement du niveau de Fermi. Nous trouvons un bon accord quantitatif entre la théorie et l'expérience pour les forts dopages ($n > 1{,}5 \times 10^{20}$ cm^{-3}). Pour les faibles dopages ($n < 1{,}5 \times 10^{20}$ cm^{-3}), le modèle prédit une transition magnétique du premier ordre. Ce modèle ne considérant que les interactions magnétiques montre qu'il devient énergétiquement favorable pour les électrons de créer des polarons magnétiques à $T > 40$ K. Une transition métal-isolant apparaissant alors au voisinage de cette température supprime le mécanisme d'échange indirect et la transition magnétique du premier ordre qui lui est associée.

Abstract. — The influence of free carriers concentrations on magnetic properties of EuO single crystals has been studied. Increasing electronic concentrations from quasi stoichiometric EuO have been achieved by departure from stoichiometry (Eu rich EuO) and by doping (2 % Gd doped EuO). The magnetization of bulk samples, characterized by transport measurements, has been measured with a vibrating sample magnetometer. For low doping, magnetization curves do not depart from the Brillouin law, with a Curie temperature $T_c = 69.4$ K. On the contrary, for heavily Gd doped sample, T_c increases up to 143 K and the reduced magnetization is smaller than that expected from the Brillouin law. We propose a model taking into account both the superexchange interaction which explains the magnetic behaviour of insulating EuO and an indirect exchange due to the conduction electrons in semiconducting and metallic samples. The main feature is that, contrary to usual models we take into account the carrier statistics, i.e. splitting of spin subbands and spread out of the Fermi level. There is a good quantitative agreement between theory and experiment for heavy doping ($n > 1.5 \times 10^{20}$ cm^{-3}). For a low doping ($n < 1.5 \times 10^{20}$ cm^{-3}), the model predicts a first order magnetic transition. This model, considering only magnetic interactions, shows that it becomes energetically favourable for the electron system to create bound magnetic polarons at $T > 40$ K. Then a metal insulator transition occurring near this temperature suppresses the indirect exchange mechanism and the correlated first order magnetic transition.

1. **Introduction.** — Europium oxide is a magnetic semiconductor in which the highest valence states are made up of the 4f electrons of Eu^{2+} on a localized level, while the bottom of the conduction band is built with s or d states [1-2]. Stoichiometric EuO is an insulator and the ferromagnetism is due to the direct superexchange interaction between localized spins $S = 7/2$ of the 4f electrons.

The introduction of carriers in the conduction band by departure from stoichiometry or by doping gives a semiconductor or metallic character to the samples and is responsible for an additional indirect d-f exchange interaction [3-4]. The study of these magnetic interactions are of great interest because they are considered as responsible for some noticeable specific properties of EuO : first, for a moderate doping, like Eu doping due to unstoichiometry, a metal-insulator transition (M.I.T.) [5] occurs below T_c, which has been ascribed to the formation of a bound magnetic polaron [6], i.e. a trapping of the electrons resulting mainly from an exchange energy gained by locally ordering the spin of the electron with the localized 4f spins of Eu atoms around the oxygen vacancy.

Second, for a heavy doping, a large increase of the Curie temperature has been observed, attributed to the indirect exchange interaction [7], together with a strong deviation of the magnetization from the Brillouin law [8-9].

In this paper, we propose a model to calculate the indirect exchange interaction outlined in reference [10]. The model relies on some approximations [10], the most drastic ones being the molecular field approximation, and the fact that interactions between the carriers and the compensating charges are averaged out. In compensation, the calculations take into account the following specific features of the material, not considered in the classical models which are then inadequate in the present case. *a*) The electron gas is not completely degenerate at all temperatures of interest. That is why the indirect exchange is calculated explicitly at finite temperature T rather than at $T = 0$. *b*) In the ferromagnetic configuration, the atomic exchange is not small compared with the Fermi energy E_F measured from the bottom of the conduction band, and the model takes into account the subsequent important polarization of the electron gas. *c*) The conduction bandwidth ($\simeq$ 1 eV) is small, and we then found it necessary to account for the finitude of the conduction bandwidth by a suitable dispersion law different from that of free electrons. These features, which are not usually met with in metals induce strong deviations from the Ruderman-Kittel-Kasuya-Yosida interaction and imply distinct magnetic properties on both sides of a temperature T_0 at which the spin down subband becomes populated. The model also leads to the existence of a critical electron concentration $n_c \simeq 1.5 \times 10^{20}$ cm^{-3}, which separates the case of a heavy doping (i.e. $n > n_c$) without discontinuities of the physical properties from the case of a low doping ($n < n_c$), characterized by instability phenomena such as a first order ferro to paramagnetic transition approaching a metal-insulator transition.

Comparing theory with experiments we report in this paper transport and magnetic measurements on three single crystal EuO samples. Sample 1 is an insulating quasi stoichiometric sample. Sample 2 is an Eu rich EuO with $n \lesssim n_c$. It is not possible to get higher electron concentrations on single crystal samples by a departure from stoichiometry contrary to the case of thin films; that is why sample 3 with $n > n_c$ is a Gd-doped EuO sample. The gadolinium has been chosen because the spin of Gd^{3+} is the same as that of Eu^{2+}, i.e. 7/2, so that any alloying effect is expected to be small, and will be neglected. Previous experimental measurements of the magnetization were deduced from magneto optical measurements on thin films [7, 8, 9]. On the contrary, we report here magnetization curves measured with a Foner type vibrating sample magnetometer on bulk samples, which allowed us to avoid any surface effect and to deal with a crystalline and homogeneous material.

Experiments are reported in section 2. In section 3 we develop the model and section 4 is devoted to the discussion of the results. Quite good quantitative agreement with experiment is found for high doping. For small doping, we provide further enlightenment of the metal insulator transition in EuO in the ferromagnetic configuration.

2. **Experiments.** — 2.1 PREPARATION TECHNIQUES. — EuO single crystals have grown by the techniques of Guerci-Shafer [11]; this has been described elsewhere [12]. A melting bath of compound is slowly cooled (3.6 °C/h) in a sealed molybdenum crucible. The sample's homogeneity is insured by two meltings of the compound with an intermediate recovery of the crucible. The initial concentrations of europium sesquioxide and metallic europium which have been used correspond respectively to $Eu_{1.024}O$ and $Eu_{1.033}O$ for the nearly stoichiometric sample and for Eu rich EuO. Gd doped EuO have been grown with the same techniques, the initial concentrations corresponding to $Eu_{1.000}Gd_{0.020}O_{1.000}$; doping with Gd is realized by adjunction of metallic Gd. Lattice constants have been measured on powder diagrams and are respectively 5.143 Å for samples 1 and 2 and 5.136 Å for sample 3. These values are nearly the same as those (5.143 Å and 5.135 Å) [13, 14] measured on crystals of the same kind; no other rings than those of EuO appear. Metallographic, electronic and X-ray pictures do not reveal the existence of several phases or clusters of metallic Gd. Microprobe analysis gives a Gd concentration of 1.5 $\pm$ 0.5 at. %.

2.2 ELECTRIC AND MAGNETIC MEASUREMENTS. — 2.2.1 *Electric measurements.* — The samples have also been characterized by measurement of their

electrical resistivity in the whole range (20-300 K) and comparison with the results of Shafer, Torrance, Penney [15]. YbAg contacts have been deposited on sample 1; on samples 2 and 3 ultrasonic indium contacts are used for electrical and Hall measurements.

The resistivity of sample 1 at 300 K is 9×10^7 Ωcm and exhibits with temperature a semiconductor type behaviour with an activation energy of 500 meV, without insulator metal transition at 50 K. On this sample optical absorption measurements have been performed to complete the characterization after polishing and thinning down to 200 μ. The absorption coefficient (ratio of optical density with sample thickness) at $\lambda = 2\,\mu$, measured at 300 K, is 50 cm^{-1}. This value is slightly larger than that for a stoichiometric sample; nevertheless no absorption peak around 2 μ is observed. This nearly stoichiometric sample is then slightly rich in Eu. For the three samples we give in figure 1 the variation of resistivity with temperature. The values of carrier concentrations and mobilities, derived from measurements of resistivity and Hall effect are reported in table I. The electron concentration as measured at 300 K for sample 3 $n \simeq 8 \times 10^{20}$ cm^{-3}, is in rather good agreement with the concentration of Gd atoms, which can then be considered as all ionized at this temperature. The electron concentration of sample 2 in the metallic state is lower, namely 1.6×10^{20} cm^{-3} but is almost equal to the critical concentration calculated in the model.

2.2.2 *Apparatus for magnetic measurements.* — Magnetization measurements with a Foner type vibrating sample magnetometer requires a particular cryostat such as that described in reference [16] (referred (M) in this paper), supplied with an interior

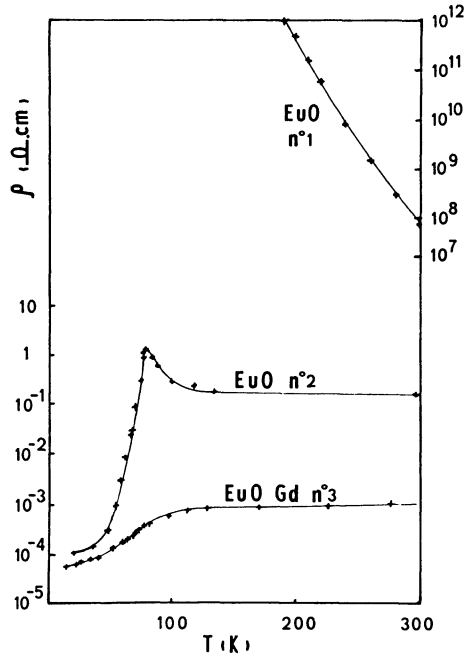

FIG. 1. — Resistivity ρ *vs.* temperature T for sample 1 (right scale), and samples 2 and 3 (left scale).

TABLE I

Transport properties of samples 2 *and* 3

	T (K)	n (cm^{-3})	ρ (Ω cm)	μ (cm^2/Vs)
EuOGd	300	8.2×10^{20}	10^{-3}	8
n° 3	180	4.8×10^{20}	9×10^{-4}	14
	40	1.9×10^{20}	7×10^{-5}	480
EuOEu	300	5.1×10^{19}	0.17	0.7
n° 2	20	1.6×10^{20}	1.1×10^{4}	340

chamber (L) to get low temperature results. Usually, thermometers are placed near to the sample. This is a severe limitation since it prevents us from using very sensitive thermometers with a significant magnetic susceptibility. That is why we have designed a vibrating rod with thermometers outside the sensitive region of the pick up coils to get an accurate measurement of the temperature over the whole range of interest (1.6-300 K), without affecting the accuracy of the magnetization measurement. The lower rod section is shown in figure 2. The lower end of the sample drive rod is glued with araldite to a tube 4 mm outside diameter and 0.5 mm thick (B) machined from dural, i.e. Al (4 % Cu) alloy. A teflon buffer ring (K) is used to prevent friction with the interior walls of the cryostat. The sample holder (I) is stirrup-shaped so that we

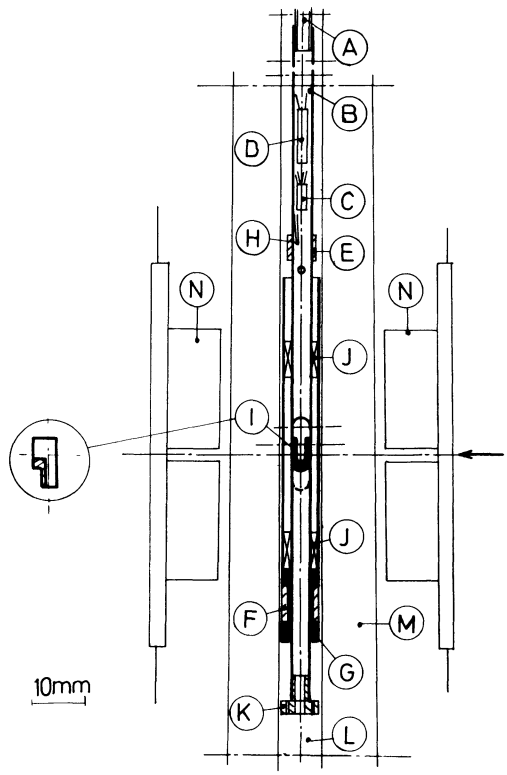

FIG. 2. — Lower section of the sample drive rod. Significance of the letters are indicated in the text. The arrow points out the magnetic field direction. The bit I in the circle is a vertical cross section perpendicular to that of the whole figure.

could set our parallelepiped ferromagnetic sample with the long side parallel to the magnetic field axis (this is the geometric configuration leading to the lowest demagnetizing field). The sample holder is enclosed in a removable dural sleeve fitting 0.6 mm outside diameter and 0.3 mm thick (G) which fits on two machined dural rings (J) rigidly fixed to the rod (B) on both sides of the sample, in order to homogenize the temperature around the sample. The heat is generated by two heater coils connected in series. One of them (F) at the lower end of the dural sleeve fitting is a 260 Ω resistance. The other one (E) is a 150 Ω resistance wound round the sample rod (B) near the upper end of the sleeve fitting. The ratio of the two resistances has been chosen to limit temperature gradients along the rod near the sample. The temperature regulation is achieved with a Au (0.03 % Fe) chromel thermocouple (H) in the true vicinity of the 150 Ω heater, and allows us to hold steady the desired temperature level while taking measurements (15 minutes). The temperature sensors are set outside the sensitive region of the pick up coils (N). This allows us to choose a Ge diode (C) in spite of its high magnetic susceptibility to measure low temperatures ($1.6 < T < 77.3$ K). A Pt thermometer (D) manufactured by Scientific Instruments is used to measure higher temperatures. All thermometers, thermocouple and heating coils are held in place with Ge-7031 thermosetting varnish. Their threads pass in the bore of inox tubes, and are soldered to a Deutsch connector which locks into the transductor assembly. However, these temperature sensors are not mounted close to the sample, so that the temperature at the thermometer sites is not the same as at the sample level. To measure the temperature T'' at the sample site *vs.* the temperature T' as given by the thermometer sensors set on the rod, we have replaced the sample by another Pt thermometer. For $T'' < 77.3$ K, the sample is first cooled by introducing liquid helium in the cryostat. The desired temperature is then reached with the use of the heating coils. The temperature T' is given by the Ge diode. A difference between T' and T'' appears at a temperature $T > 14$ K and is given by :

$$T'' - T' = 0.036 \times T' - 0.5 . \qquad (2.1)$$

For $T > 77.3$ K, the same procedure is used but liquid helium is replaced by liquid nitrogen. However thermal exchange gas in chamber L is always helium gas. T' is now measured with the Pt thermometer. The difference between T' and T'' becomes significant at $T > 79$ K and is given by :

$$T' - T'' = 0.172 \times T' - 13.6 . \qquad (2.2)$$

Reproductible results are only obtained when the heater voltage is increased in small steps (corresponding to an increase of $\sim$ 5 K) from 4.2 K at 77 K. Moreover sufficient time (10 minutes) must be allowed for the quasi steady state to be reached at each new temperature. The accuracy of the sample temperature determination is $\Delta T \leqslant 1$ K in the range [4.2-77 K] and < 1.5 K for $T > 77$ K. The contribution of the designed rod and sample holder to the magnetic moment of the samples studied on the magnetometer is 10^{-3} emu at ambiant temperature, 5×10^{-3} emu at 77 K and 4.2 K, at a magnetic field 1 T, which is negligible for our samples.

2.2.3 *Magnetic measurements.* — Our samples were not ellipsoids, but parallelepipeds. Theoretically in such a case, the internal field H_{int} is not uniform inside the sample. Nevertheless, the magnetization as a function of the external field H_{ext} satisfied the linear law $H_{ext} = NM$ at low fields, with a factor $N \simeq 2$ measured at 4.2 K in quite good agreement with the theoretical value for an ellipsoid with axes equal to the length and width of the sample. This allowed us to assimilate the sample to an ellipsoid and neglect inhomogeneities of H_{int}. The effective contribution of each localized spin to the magnetization deduced from the saturation magnetization at 4.2 K was 6.8 μ_B where μ_B is the Bohr magneton, which is the expected value for the Eu^{++} ion. Experimental curves are reported in figure 3 for the three samples investigated. The values of the reduced magnetization σ have been measured every 7 K up to T_c. The contribution of the free electron gas to the magnetization of the samples being negligible, the reduced magnetization σ is also the spin polarization.

For samples 1 and 2, the magnetization curve coincides with the classical Brillouin law :

$$\sigma = B_S\left(\frac{3\,\sigma S}{S+1}\,\frac{T_c}{T}\right) \qquad (2.3)$$

where the Curie temperature is $T_c \simeq 69.5$ K. B_S is the Brillouin function. However, the magnetization curve for sample 3 is completely different. The Curie

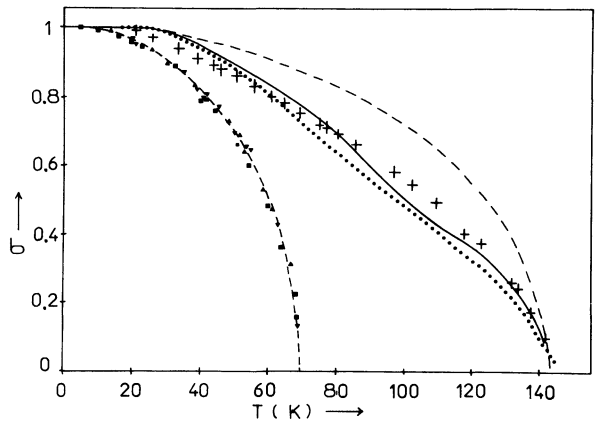

FIG. 3. — Reduced magnetization σ *vs.* temperature T. Experimental points noted ■ for sample 1, ▲ and ▼ for sample 2, and + for sample 3. We have also reported for comparison the results of 0. Massenet *et al.* [8] for an Eu rich EuO film (dotted curve). Dashed curves are Brillouin curves with $T_c = 69.5$ K and 148 K. The full curve is the result of our model for $n = 5 \times 10^{20}$ cm^{-3}.

temperature is raised to $T_c \simeq 143$ K. It is worth noticing that the highest Curie temperature reported till now for Gd-doped bulk samples in the literature was [7] 135 K for a Gd concentration $x \sim 3.4\,\%$: a possible interpretation is that the maximum of the curve T_c *versus* x occurs at a concentration x smaller than 3.4 %.

Aiming at a comparison of results, we have also reported the magnetization curve of an Eu rich EuO thin film published in reference [8], for which $T_c = 148$ K. Since this Curie temperature is practically the same as that of our sample, we should expect the curves σ *vs.* T/T_c to be superimposed. Such is not the case and the differences, even small, cannot be ascribed to experimental uncertainties. This is not surprising since, for thin films, surface effects as well as inhomogeneities may be important, and methods of measurements are different. In particular, Eu clusters present in thin films are expected to affect their magnetic properties. Let us now investigate the theoretical grounds on which this behaviour for doped and unstochiometric EuO can be understood.

---

3. **Indirect exchange model.** — In a second quantization formalism, the spin dependent part of the interaction between a conduction electron with a spin 1/2, and f electrons with a spin S is :

$$\mathcal{H}_{ex} = -\frac{J_{df}}{2N_0}\sum_j \sum_{\mathbf{k},\mathbf{q}} e^{-i\mathbf{q}.\mathbf{R}_j}\{S_j^z(c^+_{\mathbf{k}+\mathbf{q}\uparrow}c_{\mathbf{k}\uparrow} - c^+_{\mathbf{k}+\mathbf{q}\downarrow}c_{\mathbf{k}\downarrow}) + S_j^- c^+_{\mathbf{k}+\mathbf{q}\uparrow}c_{\mathbf{k}\downarrow} + S_j^+ c^+_{\mathbf{k}+\mathbf{q}\downarrow}c_{\mathbf{k}\uparrow}\} \tag{3.1}$$

J_{df} is the local atomic d-f exchange, S_n is the spin of the f electron on site R_n, N_0 is the number of Eu atoms. c_k^+ and c_k are creation and anihilation operators of a conduction electron with a wave vector $\mathbf{k}$. To the first order in the perturbation theory, only the diagonal term is considered and the energy of the carriers is :

$$E(\mathbf{k})^{\pm} = E^0(\mathbf{k}) \mp \frac{1}{2}J_{df}\,S\sigma\,. \tag{3.2}$$

This is the result of Fröhlich and Nabarro [17]. $E^0(\mathbf{k})$ is the unperturbed energy of the carriers, $E(\mathbf{k})^+$ refers to a carrier with a spin up and $E(\mathbf{k})^-$ to a spin down. The second order Hamiltonian $\mathcal{H}'_{ex}$ is deduced from the diagonal part of eq. (3.1) :

$$\mathcal{H}'_{ex} = \left(\frac{J_{df}}{2N_0}\right)^2 \sum_{ij}\sum_{\mathbf{k},\mathbf{q}} e^{i\mathbf{q}.(\mathbf{R}_i-\mathbf{R}_j)}\left\{S_i^z S_j^z \times \frac{c^+_{\mathbf{k}\uparrow}c_{\mathbf{k}+\mathbf{q}\uparrow}c^+_{\mathbf{k}+\mathbf{q}\uparrow}c_{\mathbf{k}\uparrow} + c^+_{\mathbf{k}\downarrow}c_{\mathbf{k}+\mathbf{q}\downarrow}c^+_{\mathbf{k}+\mathbf{q}\downarrow}c_{\mathbf{k}\downarrow}}{E^0(\mathbf{k}) - E^0(\mathbf{k}+\mathbf{q})} + \right.$$

$$\left. + S_i^- S_j^+ \frac{c^+_{\mathbf{k}\uparrow}c_{\mathbf{k}+\mathbf{q}\downarrow}c^+_{\mathbf{k}+\mathbf{q}\downarrow}c_{\mathbf{k}\uparrow}}{E(\mathbf{k})^+ - E(\mathbf{k}+\mathbf{q})^-} + S_i^+ S_j^- \frac{c^+_{\mathbf{k}\downarrow}c_{\mathbf{k}+\mathbf{q}\uparrow}c^+_{\mathbf{k}+\mathbf{q}\uparrow}c_{\mathbf{k}\downarrow}}{E(\mathbf{k})^- - E(\mathbf{k}+\mathbf{q})^+}\cdot\right\} \tag{3.3}$$

When the populations of the up and down spin subbands are equal, the commutation properties of c_k^+ and c_k allow us to express $\mathcal{H}'_{ex}$ as follows :

$$\mathcal{H}'_{ex} = \left(\frac{J_{df}}{2N_0}\right)^2 \sum_{i,j}\mathbf{S}_i.\mathbf{S}_j \sum_{\mathbf{k},\mathbf{q}} \frac{n_{\mathbf{k}}(1-n_{\mathbf{k}+\mathbf{q}})}{E^0(\mathbf{k}) - E^0(\mathbf{k}+\mathbf{q})} e^{i\mathbf{q}.(\mathbf{R}_i+\mathbf{R}_j)} \tag{3.4}$$

n_k is the occupation number. This is the basic relation of the Ruderman-Kittel-Kasuya-Yosida (RKKY) theory. The RKKY model thus implies the neglect of the electron gas polarization. Moreover further approximations are made in following calculations of the model such as mean field approximation, neglect of thermal effects by assuming $T = 0$, neglect of the finitude of the conduction band width.

On the contrary, in the ferromagnetic configuration, at sufficiently low temperatures, the spin splitting of the conduction band $J_{df}\,S\sigma$ is larger than the Fermi energy E_F for electron concentrations of interest ($n < 10^{21}$ cm^{-3}) so that only the spin-up subband is populated. This makes the RKKY model and eq. (3.4) inadequate and we must use eq. (3.3). We shall also limit ourselves to the mean field approximation which amounts to neglecting transverse and longitudinal fluctuations, and thus drop the terms $S_i^- S_j^+$ and $S_i^+ S_j^-$ in eq. (3.3). Provided with a suitable dispersion law, eq. (3.3) becomes, after integration over angular variables [10] :

$$\left.\begin{aligned} J_{eff}(R_{ij}) &= -\frac{8}{W}\left(\frac{VJ_{df}}{4\pi^2 N_0 R_{ij}}\right)^2 \mathfrak{I}\int_0^{\pi/a} dk(n_{k\uparrow} + n_{k\downarrow})\,k\sin(kR_{ij}) \times \int dk' \frac{k'\sin k' R_{ij}}{\cos k' a - \cos ka} \\ a &= \left(\frac{\pi}{3}\right)^{1/3}\frac{a'}{2} \end{aligned}\right\} \tag{3.5}$$

V is the volume of the crystal, and a' the lattice parameter. $\mathcal{F}$ means the Cauchy principal part of the integral. The calculation of the integral is reported in the appendix. The final expression for $J_{\text{eff}}(R_{ij})$ is :

$$J_{\text{eff}}(R_{ij}) = -\frac{2}{W}\left(\frac{VJ_{\text{df}}}{2\pi^2 N_0 R_{ij}}\right)^2 e^{-R_{ij}/\lambda}\left\{\sum_{\substack{m=-\infty \\ m\neq 0}}^{m=+\infty}(-1)^m \times \left\{\frac{\sin(\pi R_{ij}/a)}{(R_{ij}+ma)^2} - \frac{\pi}{a}\frac{\cos(\pi R_{ij}/a)}{R_{ij}+ma}\right\} \times \right.$$

$$\left. \times \int_0^{\pi/a} \left\{ f\left(E^0(k) + \frac{J_{\text{df}}\, S\sigma}{2}\right) + f\left(E^0(k) - \frac{J_{\text{df}}\, S\sigma}{2}\right)\right\} \frac{k \sin(kR_{ij}) \sin(mka)}{\sin(ka)}\, dk \right\} \qquad (3.6)$$

$f(E)$ is the Fermi function. We have introduced the exponential factor $e^{-R_{ij}/\lambda}$ taking into account that the mean free path λ of the electrons is finite [18]. This induces a cut-off of the indirect exchange because an electron cannot couple magnetic spins distant by more than the mean free path. λ is related to μ according to the law $\lambda = \frac{\hbar}{e}\mu k_F$ where e is the electron charge and k_F the wave vector at the Fermi level. In the molecular field approximation, σ is given by :

$$\sigma = B_S\left\{\frac{\sigma S^2\{I(0) + J_{\text{eff}}(0)\}}{k_B T}\right\} \qquad (3.7)$$

k_B is the Boltzmann constant. $I(0)$ and $J_{\text{eff}}(0)$ are the Fourier transforms at $q = 0$ of the direct and indirect exchange constants respectively. The elaborate and unclassical expression of the indirect exchange in eq. (3.6) is of course the consequence of the features of the model which are usually neglected : the thermal effects and non degeneracy of the electron gas are responsible for the presence of Fermi functions instead of Dirac functions. Because of the electron gas polarization $J_{\text{df}}\, S\sigma/2$ cannot be neglected in the arguments of the Fermi functions, so that $J_{\text{eff}}(R_{ij})$ depends on σ. Since σ also depends on $J_{\text{eff}}(0)$ according to eq. (3.7), both $J_{\text{eff}}(0)$ and σ are solutions of the set of eqs. (3.6) and (3.7) which must be solved self consistently. Finally, the departure from a free electron dispersion law and the correlated finitude of the conduction bandwidth are responsible for the complex dependence of $J_{\text{eff}}(R_{ij})$ on R_{ij}. The chosen parameters are :

$$J_{\text{eff}} \simeq 0.13 \text{ eV [19]}, \quad I(0) = 1.14 \times 10^{-3} \text{ eV [20]}$$

and

$$W \simeq 1.1 \text{ eV [1]}.$$

Let T_0 be the temperature at which the Fermi energy is equal to the spin splitting, i.e. $E_F = J_{\text{eff}}\, S\sigma$. Quite different results are obtained depending on the sign of ΔJ_{eff} defined as the difference between $J_{\text{eff}}(0)$ at $T = T_c$ and $J_{\text{eff}}(0)$ at $T = T_0$. In effect, $J_{\text{eff}}(0)$ like T_c being strongly increasing functions of n in the paramagnetic configuration [10]. $\Delta J_{\text{eff}}(0)$ is negative

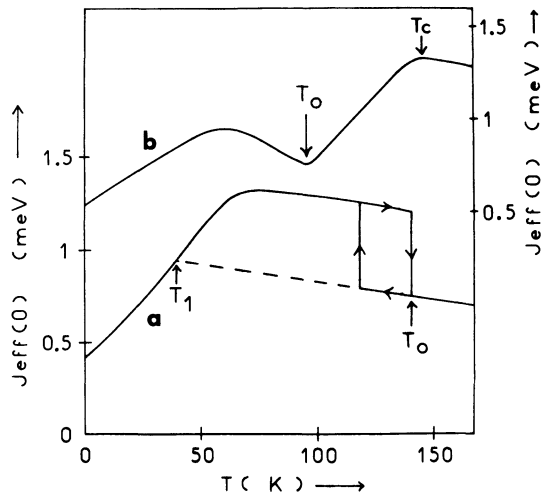

FIG. 4. — Fourier transform of the indirect exchange constant at $q = 0$, $J_{\text{eff}}(0)$, as a function of temperature for electron concentrations $n = 1.3 \times 10^{20}$ cm^{-3} (curve a, left scale) and $n = 5 \times 10^{20}$ cm^{-3} (curve b, right scale). The broken curve represents variations of $J_{\text{eff}}(0)$ calculated with a spin polarization $\sigma = 0$ when smaller than $J_{\text{eff}}(0)$ calculated self consistently ($\sigma \neq 0$). The temperatures T_0 and T_1 are referred to in the text.

at low concentrations and goes through zero at a concentration n_c which in our model is

$$n_c \simeq 1.5 \times 10^{20} \text{ cm}^{-3}.$$

The variation of $J_{\text{eff}}(0)$ *vs.* T is illustrated in figure 4 for concentrations $n = 1.3 \times 10^{20}$ cm^{-3} and

$$n = 5 \times 10^{20} \text{ cm}^{-3}$$

on both sides of n_c.

In the case $n < n_c$, the fact that $\Delta J_{\text{eff}}(0) < 0$ is related to the existence of a temperature $T_1 < T_0$ beyond which the indirect exchange coupling is increased (and the exchange energy decreased) by an alignment of the magnetic spins. In other words, the value of $J_{\text{eff}}(0)$ calculated with the assumption $\sigma = 0$ is lower than the value deduced by solving eqs. (3.6) and (3.7) with $\sigma \neq 0$ in the range $T_1 < T < T_0$. Considering only magnetic interactions, it then becomes energetically favourable for the electrons to remain localized around the Gd impurities, so as to align their spins with the spins of neighbouring Eu

atoms. In such a case, the metallic state is no longer stable with respect to the formation of bound magnetic polarons in an insulating state [6]. Then eqs. (3.6) and (3.7) become irrelevant because they have been established assuming *a priori* that the ground state of the electron system is a free electron gas. At $T < T_1$, our calculations remain valid but at $T \simeq T_1$, the system undergoes a metal insulator transition, and at higher temperatures, the magnetization is that of pure insulating EuO and vanishes at $T_c \simeq 69$ K.

Let us however investigate which magnetic properties the material would have if the electrons were always in conduction states. In such a case, a consequence of the inequality $\Delta J_{eff}(0) < 0$ is that at $T = T_0$, the increase of the spin disorganization with T is further increased by a reduction of the indirect exchange coupling; this increases the ferro to paramagnetic transition which becomes of the first order. This transition does not occur at the same temperature whether we approach it from the ferro or from the paramagnetic side. In effect, there exists a range of temperatures in which eqs. (3.6) and (3.7) have a solution for $J_{eff}(0)$ and σ corresponding to a ferromagnetic configuration with only the spin up subband populated (large value of $J_{eff}(0)$) and another solution with $\sigma = 0$ (low value of $J_{eff}(0)$) corresponding to a paramagnetic configuration. The ferromagnetic configuration exists until the temperature is high enough for the spin down subband to be also populated. Thus, the system undergoes a transition from the ferro to the paramagnetic state at $T_c = T_0$. The paramagnetic solution exists until the temperature becomes lower than the paramagnetic Curie temperature which is given by :

$$\theta = \frac{S(S+1)}{3\,k_B}\{\, I(0) + J_{eff}(0)\,\}$$

in our molecular field approximation. These results are illustrated in figure 5.

On the contrary, in the case $n > n_c$, the metallic state is always stable, eqs. (3.6) and (3.7) being valid at all

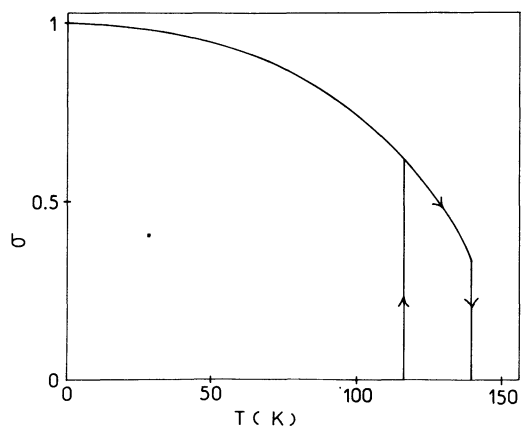

FIG. 5. — Reduced magnetization μ *vs.* temperature T for an hypothetic EuO sample with a free electron concentration $n = 1.3 \times 10^{20}$ cm^{-3} at all temperatures.

temperatures. Since $\Delta J_{eff}(0) > 0$, $J_{eff}(0)$ is larger in the paramagnetic configuration than in the ferromagnetic one, an increase of T near T_c in the ferromagnetic configuration produces an increase of the thermal spin disorganization which is counterbalanced by an increase of the indirect exchange coupling. Owing to the opposition of these two effects, the transition is only of the second order.

4. **Discussion.** — With experimental magnetization curves, we have also plotted in figure 3 the theoretical curve for an electron concentration $n = 5 \times 10^{20}$ cm^{-3} deduced from Hall effect measurements just above T_c for sample 3. A quite good agreement is found between theory and experimental data for this sample as well as for the film studied in reference [8]. Within our model, the large deviation of the curves from the Brillouin law, already outlined in reference [8], can be understood as follows : at low temperatures up to $T_0 \simeq 90$ K, only the spin up subband is populated. According to the values of $J_{eff}(0)$ in such a case, we should expect a Curie temperature $T_c \simeq 100$ K. Then at $T > T_0$, $J_{eff}(0)$ increases strongly for the reasons described in the previous section, as can be seen in figure 4. This leads to an increase of the Curie temperature which is raised up to $T_c = 143$ K.

On the other hand, according to our model, the amplitude of the magnetic circular dichroism of such a sample with such an electron concentration, as temperature decreases, should increase rapidly below 140 K, saturate below 100 K and increase again when decreasing T from 80 K to lower temperatures. This is exactly the result reported on a EuO thin film by Ferre *et al.* [9]. However, the lack of information concerning the homogeneity, stoichiometry, and electron concentration of this film prevents us from regarding their data as definite grounds for the validity of our model.

For sample 2, the M.I.T. occurs at $T \simeq 50$ K in fairly good agreement with our predicted value $T_1 = 40$ K. At this temperature, the magnetization is still large ($\sigma \simeq 0.8$) and not yet very different from that of pure EuO at the same temperature. This is why the magnetization curve of such samples may be approximated by the Brillouin law at all temperatures as for pure EuO. Since at $T > 50$ K the sample is in an insulating configuration, the indirect exchange is smeared out and $T_c \simeq 69$ K as for sample 1. We then expect a discontinuity of the Curie temperature as a function of n at the critical concentration n_c where T_c is suddenly raised to about 110 K. This agrees with experiments reported by Samokhvalov *et al.* [21] and not with those reported by Schoenes *et al.* [22]. We can also notice that it is not possible by magnetization measurements to distinguish between a metal insulator transition induced by a change of the electron concentrations or by a change of the mobility of the free carriers. In effect, in the latter, case, the indirect

exchange is cancelled owing to the exponential factor in eq. (3.6).

Contrary to classical theories, our model accounts for the various magnetic properties of Gd doped and undoped EuO. Three specific features of the model outlined above are needed for this overall agreement with experiment. For example, it was necessary to take into account the finitude of the conduction bandwidth to account quantitatively [10] for the variations of the Curie temperature with the electron concentration [7, 8]. We have accounted [10] for the anomalous value of the Curie constant, a few % smaller than expected from usual models, as deduced from susceptibility measurements in the paramagnetic configuration [23], because we have taken into account the spreading of the Fermi distribution. We have accounted for the shape of the magnetization curves for high electron concentration, different from the Brillouin curves, because we have taken into account the polarization of the electron gas. These two last aspects of the carrier statistics were responsible for the existence of a metal insulator transition at $T \simeq 50$ K for $n \simeq 1.5 \times 10^{20}$ cm^{-3} as experimentally observed. This shows that the indirect exchange mechanism between 4f spins, which has not been considered in the theories of the metal-insulator transition [6] has a great importance in the formation of the bound magnetic polarons, which may be one reason for which the model proposed by Leroux Hugon [6], contrary to experiments, does not lead to results significantly different from the usual Mott transition.

5. **Conclusion.** — The influence of free carrier concentrations on magnetic properties of EuO has been investigated. Our model led us to separate the case of a heavy doping $n > 1.5 \times 10^{20}$ cm^{-3} and that of a low doping $n < 1.5 \times 10^{20}$ cm^{-3}. The theory fully accounts for the magnetic properties of samples with $n > 1.5 \times 10^{20}$ cm^{-3}. In this case, the similarity of the magnetization curves for EuO samples with free electrons introduced by substitution of Gd^{3+} to Eu^{2+} or by non stoichiometry corroborates that the particular deviation from the Brillouin law is due to the electron gas rather than to some disorder effect [8] which should depend on the nature of the defects. To insure the validity of this purpose, the study of a Gd doped EuO sample with an electron concentration similar to that of sample 2 is under study at the present time. In the case of a low doping, a metal insulator transition prevents a first order ferroparamagnetic transition to occur, and magnetization curves do not depart from the classical Brillouin law.

We can then conclude that for such a heavy doping, the average magnetization has a strong effect on the free electrons, but in turn, the level crossing in the electronic system, also greatly affects the average magnetization curve, which becomes similar to that of a two component material. In the case of a low doping, although the influence of the average magnetization on the free electrons is always very great (inducing a M.I.T.), the free electrons do not exert a significant influence on the magnetization. It is clear that much more accurate thermodynamic calculations, taking into account not only magnetic interactions but also kinetic and Coulomb energies, are required to study the metal insulator transition in detail. We have shown that it will be important in such a study to take into account statistical effects on the indirect exchange, and to perform the calculations explicitly at a finite temperature. This study is in progress at the present time and should provide a better understanding of the bound magnetic polaron.

Appendix A. — In this Appendix, we show how to calculate the integral :

$$I = \mathcal{P} \int_0^{\pi/a} \frac{k' \sin (k' R_{ij})}{\cos (k' a) - \cos (ka)} \, dk' \qquad (A.1)$$

which appears in the expression of the indirect exchange coupling constant $J_{\text{eff}}(R_{ij})$ in eq. (3.5). To avoid the pole, we can write :

$$I = \frac{I_+ + I_-}{2} \qquad (A.2)$$

$$I_\pm = \lim_{\varepsilon \to 0} \int_0^{\pi/a} \frac{k' \sin (k' R_{ij})}{\cos (k' a) - \cos (ka) \pm i\varepsilon} \, dk' .$$

It is convenient to introduce the quantity μ defined by :

$$\mu = i \operatorname{cotg} (ka) + \varepsilon \sin^3 (ka) . \qquad (A.3)$$

With this notation, we can write :

$$I_+ = - \lim_{\varepsilon \to 0} \frac{\mu}{\cos (ka)} \int_0^{\pi/a} \frac{k' \sin (k' R_{ij})}{\mu - \sqrt{\mu^2 - 1} \cos (k' a)} \, dk' \qquad (A.4)$$

and a similar expression for I, μ being replaced by its complex conjugate μ^*. Since μ or μ^* are outside the real segment [0, + 1], and have a positive real part, it is possible to develop the integrant on the basis of the first kind Legendre functions P_0^m :

$$[\mu \pm \sqrt{\mu^2 - 1} \cos (k', a)]^{-1} = P_0^0(\mu) + 2 \sum_{m=1}^{\infty} (\mp 1)^m \, m \, ! \, P_0^{-m}(\mu) \cos (mk' a) . \qquad (A.5)$$

Since $P_0^0(\mu) = 1$, eq. (A.2) becomes :

$$I = - \frac{1}{\cos (ka)} \lim_{\varepsilon \to 0} \int_0^{\pi/a} dk' \, k' \sin (k' R_{ij}) \sum_{m=1}^{\infty} m \, ! \times \cos (mk' a) \left[\mu P_0^{-m}(\mu) + (-1)^m \mu^* P_0^{-m}(\mu^*)\right] . \qquad (A.6)$$

It is straightforward to deduce from the definition of the Legendre functions that :

$$P_0^{-m}(i \operatorname{cotg}(ka)) = \frac{1}{m!} e^{imka}$$
$$P_0^{-m}(-i \operatorname{cotg}(ka)) = \frac{(-1)^m}{m!} e^{-imka} \quad (A.7)$$

so that eq. (A.6) can be written :

$$I = \frac{2}{\sin(ka)} \int_0^{\pi/a} dk' \, k' \sin(k' R_{ij}) \times \sum_{m=1}^{\infty} \sin(mka) \cos(mk' a) .$$

The integration can then be easily achieved and leads to :

$$I = \sum_{m=1}^{\infty} (-1)^m \left[\frac{\sin(\pi R_{ij}/a)}{(R_{ij} + ma)^2} - \frac{\pi}{a} \frac{\cos(\pi R_{ij}/a)}{R_{ij} + ma} + (1 - \delta_{R_{ij},ma}) \left(\frac{\sin(\pi R_{ij}/a)}{(R_{ij} - ma)^2} - \frac{\pi}{a} \frac{\cos(\pi R_{ij}/a)}{R_{ij} - ma} \right) \right] \quad (A.8)$$

δ is the Kronecker symbol.

References

[1] BUSCH, G., GÜNTHERODT, G., WACHTER, P., *J. Physique Colloq.* **32** (1971) C1-928.

[2] FEINLEIB, J., SCOULER, W. J., DIMMOCK, J. O., HANUS, J., REED, T. B., PIDGEON, C. R., *Phys. Rev. Lett.* **22** (1969) 1385.

[3] RUDERMAN, M. A., KITTEL, C., *Phys. Rev.* **96** (1954) 99.

[4] KASUYA, T., *Prog. Theor. Phys.* **16** (1966) 45 ; YOSIDA, K., *Phys. Rev.* **106** (1957) 893.

[5] OLIVER, M. R., Thesis M.I.T. (1970).

[6] TORRANCE, J. B., SHAFER, M. W., MC GUIRE, T. R., *Phys. Rev. Lett.* **29** (1972) 1168 ; LEROUX HUGON, P., *Phys. Rev. Lett.* **29** (1972) 939.

[7] AHN, K. Y., MC GUIRE, T. R., *J. Appl. Phys.* **39** (1968) 5061.

[8] MASSENET, O., CAPIOMONT, Y., NGUYEN VAN DANG, *J. Appl. Phys.* **46** (1974) 3593.

[9] FERRE, J., BADOZ, J. B., PAPARODITIS, C., SURYANARAYANAN, R., *I.E.E.E. Trans. Magn. Mag.* **7** (1971) 388.

[10] MAUGER, A., *Phys. Status Solidi* **84b** (1977) 761.

[11] GUERCI, C. F., SHAFER, M. W., *J. Appl. Phys.* **37** (1966) 1406.

[12] LLINARES, C., DESFOURS, J. P., NADAI, J. P., GODART, C., PERCHERON, A., ACHARD, J. C., *Phys. Status Solidi* **25a** (1974) 185.

[13] HUBER, E. J., HOLLEY, C. E., *J. Chem. Thermodyn.* **1** (1969) 301.

[14] VON MOLNAR, S., SHAFER, M. W., *J. Appl. Phys.* **41** (1970) 1093 ; GRANT, P. M., *J. Appl. Phys.* **42** (1977) 1771.

[15] SHAFER, M. W., TORRANCE, J. B., PENEY, T., *J. Phys. Chem. Solids* **33** (1972) 2251.

[16] ESCORNE, M., LEROUX-HUGON, P., *Rev. Phys. Appl.* **8** (1973) 289.

[17] FRÖHLICH, H., NABARRO, F. R. N., *Proc. R. Soc. London* **A 175** (1940) 382.

[18] See for example MATTIS, D. C., *The theory of magnetism* (Harper and Row Ltd, London) 1965.

[19] FREISER, M. J., HOLTZBERG, F., METHFESSEL, S., PETTIT, G. O., SHAFER, M. W., SUITS, J. C., *Helv. Phys. Acta* **41** (1968) 832.

[20] KASUYA, T., *I.B.M. J. Res. Dev.* **14** (1970) 214.

[21] SAMOKHVALOV, A. A., ARBUZOVA, T. I., SIMONOVA, M. I., FAL'KOVSKAYA, L. D., *Sov. Phys. Solid State* **15** (1974) 2459.

[22] SCHOENES, T., WACHTER, P., *Phys. Rev.* **B 9** (1974) 3097.

[23] MC GUIRE, T. R. and HOLTZBERG, F., *A.I.P. Conf. Proc.* **10** (1973) 855.